HHS Public Access

Author manuscript

Nat Med. Author manuscript; available in PMC 2016 May 01.

Published in final edited form as:

Nat Med. 2015 November ; 21(11): 1272–1279. doi:10.1038/nm.3962.

Hair follicle-derived IL-7 and IL-15 mediate skin-resident memory T cell homeostasis and lymphoma

Takeya Adachi[1], **Tetsuro Kobayashi**[1,2], **Eiji Sugihara**[3], **Taketo Yamada**[4,*], **Koichi Ikuta**[5], **Stefania Pittaluga**[6], **Hideyuki Saya**[3], **Masayuki Amagai**[1], and **Keisuke Nagao**[1,2,**]

[1]Department of Dermatology, Keio University School of Medicine, Tokyo, Japan

[2]Dermatology Branch, Center for Cancer Research, National Cancer Institute, National Institutes of Health, Bethesda, MD, U.S.A.

[3]Division of Gene Regulation, Institute for Advanced Medical Research, Keio University School of Medicine, Tokyo, Japan

[4]Department of Pathology, Keio University School of Medicine, Tokyo, Japan

[5]Laboratory of Biological Protection, Department of Biological Responses, Institute for Virus Research, Kyoto University, Kyoto, Japan

[6]Laboratory of Pathology, Center for Cancer Research, National Cancer Institute, National Institutes of Health, Bethesda, MD, U.S.A.

Abstract

The skin harbors a variety of resident leukocyte subsets that must be tightly regulated to maintain immune homeostasis. Hair follicles are unique structures in the skin that contribute to skin dendritic cell homeostasis via chemokine production. We demonstrate that $CD4^+$ and $CD8^+$ skin resident memory T cells (T_{RM}), responsible for long-term skin immunity, resided predominantly within the hair follicle epithelium of unperturbed epidermis. T_{RM} tropism for the epidermis and follicles was herein termed epidermotropism. Hair follicle-derived IL-15 was required for $CD8^+$ T_{RM}, and IL-7 for $CD8^+$ and $CD4^+$ T_{RM}, to exert epidermotropism. The lack of either cytokine impaired hapten-induced contact hypersensitivity responses. In a model of cutaneous T cell lymphoma, epidermotropic $CD4^+$ T_{RM} lymphoma cell localization depended on hair follicle-derived IL-7. These findings implicate hair follicle-derived cytokines as regulators of malignant

**Correspondence should be addressed to, Keisuke Nagao M.D., Ph.D., Dermatology Branch, CCR, NCI, National Institutes of Health, Bethesda, MD 20892 USA, keisuke.nagao@nih.gov.

*Present address: Department of Pathology, Saitama Medical University School of Medicine, Saitama, Japan

AUTHOR CONTRIBUTIONS

T.A. and K.N. conceived and designed all experiments. Experiments were performed by T.A. with the assistance of T.K.; E.S. and H.S. provided *Ink4a/Arf*$^{-/-}$ mice and assisted with retroviral transduction; T.Y. assisted with immunohistochemical staining; K.I. provided *Il7*-floxed mice; S.P. provided human CTCL samples; M.A discussed data and provided administrative support; K.N. guided the project and T.A. and K.N. wrote the manuscript.

COMPETING FINANCIAL INTERESTS

The authors declare no competing financial interests.

and non-malignant T_{RM} cell tissue residence and suggest they may be targeted therapeutically in inflammatory skin disease and lymphoma.

Hair follicles are unique structures in the mammalian skin that provide a niche for keratinocyte and melanocyte stem cells[1,2]. Various leukocyte subsets localize with hair follicles[3]. We recently demonstrated that hair follicles recruit skin dendritic cells to sites of minor trauma[4]. Keratinocytes in the hair follicle infundibulum and isthmus produce the chemokines CCL2 and CCL20, recruiting myeloid cells after physical perturbation. A subset of keratinocytes in the suprabasal layer of the follicular bulge region expressed CCL8. CCL8 prevented local Langerhans cell (LC) accumulation, a mechanism that may protect bulge stem cells from excessive leukocyte infiltration[4]. These data establish that hair follicles actively promote immune homeostasis.

T cells that reside in peripheral tissues have been described in the recent years, and their importance is now well-established[5–9]. Skin resident memory T cells (T_{RM}) display an effector memory phenotype and are generated after immunological insults such as viral infection[6,8]. In the context of infection, $CD4^+$ memory T cells accumulate primarily in the dermis, whereas $CD8^+$ T_{RM} accumulate within the epidermis[7]. Both T cell subsets exhibited tropism to the hair follicles[7]. Skin T_{RM} express CD69 and CD103[10]. CD69 suppresses sphingosine-1-phosphate receptor 1 expression, preventing T cells from emigrating from lymphoid organs or other tissues into the circulation[11,12]. CD103 mediated retention of T cells in the skin likely occurs via adhesion to E-cadherin[13]. The non-migratory nature of $CD8^+$ T_{RM} has been established in parabiotic mice[8], and $CD4^+$ T_{RM} in human skin engrafted onto immunodeficient mice[14].

Infiltration of T cells into the epidermis is a prominent feature in both inflammatory and neoplastic human diseases including graft-versus host disease, drug eruptions, and cutaneous T cell lymphoma (CTCL). In fixed drug eruption, $CD8^+$ T cells attack the epidermis to cause keratinocyte cell death in the presence of the drug(s)[15]. After clinical resolution, $CD8^+$ T cells with a memory phenotype persist within the epidermis[15,16]. The majority of CTCL is caused by $CD4^+$ lymphoma cells[17]. In the classic form, mycosis fungoides, lymphoma cells of a T_{RM} phenotype infiltrate the epidermis including the follicular epithelium[18,19] and slowly accumulate and proliferate to form tumors. Such epidermis- and follicle-infiltrating T cells are termed epidermotropic T cells[20].

Given the importance of T_{RM} in conferring long-term immunological memory[6,8] and regulatory functions[13,21,22], elucidation of mechanisms that support long-term persistence in the skin may provide insight into T cell homeostasis in health and disease. Herein, we demonstrate that the epidermotropism of T_{RM} is supported by the hair follicle-derived cytokines, IL-7 and IL-15.

RESULTS

$CD4^+$ and $CD8^+$ T cells in steady state epidermis

To characterize T_{RM} in the epidermis, we prepared vertical sections of frozen skin samples taken from unmanipulated adult C57BL/6J mice, and visualized $CD4^+$ and $CD8^+$ T cells

using immunofluorescence microscopy. We routinely observed small numbers of both $CD4^+$ and $CD8^+$ T cells in follicular epithelium (Fig. 1a). Visualization of the basement membrane via integrin α_6 staining confirmed that both $CD4^+$ and $CD8^+$ T cells resided within the follicular epithelium (Supplementary Fig. 1a). Staining epidermal sheets revealed that $CD8^+$ T cells were present in both hair follicles and the interfollicular epidermis, whereas $CD4^+$ T cells were localized exclusively around hair follicles (Supplementary Fig. 1b). In flow cytometry analysis of epidermal cell suspensions, exclusion of LC and dendritic epidermal T cells enabled the identification of small numbers of $CD4^+$ and $CD8^+$ T cells, consistent with the immunofluorescence microscopy results (Fig. 1b). The number of $CD4^+$ T cells in the epidermis was comparable to that in the dermis (Fig. 1c). $CD8^+$ T cells were found exclusively in epidermal cell suspensions (Fig. 1c)[7]. Contamination of dermal leukocytes into the epidermal preparation and vice versa appeared unlikely (Supplementary Fig. 1c,d).

Phenotypic analysis suggests most of the $CD4^+$ and $CD8^+$ T cells are effector memory T cells, as assessed by CD44 and CD62L expressions, and are resident cells, by CD103 and CD69 co-expression (Fig. 1d). $CD4^+$ T cells in the epidermis expressed CD103 at slightly lower levels than those in the dermis (Fig. 1e,f). Furthermore, the ratio of $CD4^+$ $FoxP3^+$ regulatory T_{RM} were lower in the epidermis than in the dermis, suggesting that organization of $CD4^+$ T_{RM} in the two skin compartments may be differentially regulated. In this manuscript, memory T cells that reside in the epidermis and the follicles will be referred to as epidermotropic T_{RM} not to indicate their entity as a distinct T cell subset, but solely to describe their localization in the skin.

T_{RM} associate with hair follicles during epidermal entry

T_{RM} are generated during skin infection and accumulate not only at sites of primary inoculation, but also at distant sites[8,23]. To model this distribution of T_{RM}, we adoptively transferred WT splenocytes into *Rag2*$^{-/-}$ mice. After transfer into a lymphopenic environment, donor T cells undergo homeostatic proliferation, and we hypothesized that such T cells might distribute to peripheral tissues including epidermis and skin. Indeed, $CD4^+$ and $CD8^+$ T cells appeared in the epidermis of *Rag2*$^{-/-}$ recipients 10 days after transfer, and by day 14 their numbers reached levels detectable in WT mice (Fig. 1g). Donor T cells displayed effector memory and resident phenotypes (Fig. 1h), and thus represent epidermotropic T_{RM}.

Visualization of $CD4^+$ and $CD8^+$ T_{RM} during active epidermal repopulation revealed close association with hair follicles (Fig. 1i). $CD4^+$ T_{RM} initially appeared within the dermis and accumulated around hair follicles in frozen sections at day 7 after transfer and then distributed within the epidermis and dermis thereafter (Supplementary Fig. 1e). In contrast to $CD4^+$ T_{RM}, $CD8^+$ T_{RM} appeared directly within the interfollicular epidermis, and then accumulated around the hair follicles (Supplementary Fig. 1e,f). Thus, the anatomical mode of entry for $CD4^+$ and $CD8^+$ T_{RM} appears to be distinct.

Hair follicle keratinocytes express *il15* and *il7*

IL-15 and IL-7 are important cytokines that enable the generation and maintenance of memory T cells[24,25]. Our previous study revealed that hair follicle keratinocyte subsets

exhibit distinct chemokine expression profiles[4]. To determine if hair follicle keratinocytes expressed mRNA encoding IL-15 and IL-7, we sorted epidermal keratinocytes into those from interfollicular epidermis, infundibulum, isthmus, basal layer bulge and suprabasal layer bulge[4] (Fig. 2a). Similar to previously described patterns of chemokine expression[4], real-time PCR analysis revealed that both *il15* and *il7* mRNA were predominantly expressed by keratinocytes in the infundibulum and isthmus (Fig. 2b). Because most of the mouse pelage hair follicles are in telogen, we studied the vibrissae to determine if cytokines were expressed during anagen. The transient portions of anagen hair follicles did not express *il7*, but the bulb expressed low levels of *il15* (Supplementary Fig. 2a). We also analyzed cytokine mRNA expression in major leukocyte subsets in the epidermis, and found that LC, but not dendritic epidermal T cells, expressed *il15* (Supplementary Fig. 2b). Both leukocyte subsets lacked *il7* expression (data not shown).

Epidermotropic T_{RM} require hair follicle-derived cytokines

Analysis of $CD4^+$ and $CD8^+$ T_{RM} via flow cytometry revealed that both T cell subsets expressed IL-15/2Rβ and IL-7Rα (Fig. 2c,d). Given the unavailability of an animal model enabling conditional ablation of IL-15, we generated bone marrow (BM) chimeric mice to determine if epidermotropic T_{RM} were influenced by hair follicle-derived cytokines. Reconstitution of WT or *Il15*$^{-/-}$ mice with BM from *Rag2*$^{-/-}$ mice led to the generation of lymphopenic mice that either expressed (WT^{Rag}) or lacked (*Il15* KO^{Rag}) IL-15 in peripheral tissues including skin (Fig. 2e). We then transferred WT splenocytes into these BM chimeric mice and analyzed the numbers of epidermotropic T_{RM} at day 14 after transfer (Fig. 2e). The numbers of epidermotropic $CD4^+$ T_{RM} were slightly increased in recipient *Il15* KO^{Rag} mice, whereas epidermotropic $CD8^+$ T_{RM} numbers were reduced (Fig. 2f). The numbers of $CD4^+$ and $CD8^+$ T cells in the spleen were comparable in recipient *Il15* KO^{Rag} and WT^{Rag} mice (Supplementary Fig. 2c), indicating that the difference in the numbers of epidermotropic $CD8^+$ T_{RM} was due to the loss of IL-15 in skin. The numbers of epidermotropic $CD8^+$ T_{RM} were 10-fold higher than that of unmanipulated WT mice. Upregulation of IL-15 mRNA expression in keratinocytes in lethally irradiated mice may contribute to this (Supplementary Fig. 2d).

Because LC also expressed IL-15 mRNA, we studied the effect of LC depletion on epidermotropic T_{RM} utilizing two different models. Neither constitutive loss nor depletion of LC affected the numbers of epidermotropic T_{RM} (Supplementary Fig. 3a–c). Thus, hair follicle-derived IL-15 is crucial for the maintenance of epidermotropic $CD8^+$ T_{RM}.

A different approach was taken to evaluate the contribution of hair follicle-derived IL-7 because T cells failed to undergo homeostatic proliferation when transferred into *Il7* KO^{Rag} mice (data not shown). We crossed *K14*-Cre^{ERT} mice[26] with *Il7*-floxed mice to generate mice in which ablation of IL-7 in epidermis could be specifically induced in the skin of adult mice via tamoxifen injection (Supplementary Fig. 2e). Because of the potential for a continuous influx of newly generated T_{RM} that could alter total cell numbers during and after IL-7 ablation, we treated mice with FTY720, a sphingosine-1-phosphate receptor 1 inhibitor that inhibits lymphocyte egress from lymph nodes, thereby preventing the influx of endogenous T_{RM} into the epidermis (Fig. 2g). Epidermal ablation of IL-7 reduced the

numbers of both $CD4^+$ and $CD8^+$ T_{RM} 14 days after loss of IL-7, an effect that persisted for at least 28 days (Fig. 2h). The numbers of splenic T cells remained unaffected by the loss of IL-7 in the skin (Supplementary Fig. 2f). Therefore, hair follicle-derived IL-7 is required for both $CD4^+$ and $CD8^+$ T_{RM} to persist in the epidermis.

Impaired CHS responses in the absence of IL-7 and IL-15

Impaired anatomical localization of T_{RM} during the steady state in the absence of hair follicle-derived IL-15 and IL-7 might affect subsequent immune responses in the skin. To address this, we induced contact hypersensitivity (CHS) with a hapten in mice that lacked hair follicle-derived cytokines. To analyze the effect of IL-15 deficiency in the context of $CD8^+$ T_{RM}, we generated WT^{Rag} and *Il15* KO^{Rag} mice via BM transplantation (Fig. 2e). These BM chimeric mice were injected with $CD8^+$ T cells obtained from skin draining lymph nodes of 1-fluoro-2,4-dinitrobenzene (DNFB)-sensitized mice (Fig. 3a). Transferred $CD8^+$ T cells are expected to undergo homeostatic proliferation and distribute to peripheral tissues including skin in WT^{Rag}, but not in *Il15* KO^{Rag} mice (Fig. 1h, 2e). Recipient mice were then challenged with DNFB and ear-swelling responses were monitored. Ear swelling and lymphocytic infiltration were reduced in the absence of tissue-derived IL-15 (Fig. 3b,c).

The role of hair follicle-derived IL-7 and T_{RM} was assessed in the context of $CD4^+$ T cell-mediated CHS. To generate lymphopenic mice that constitutively lack IL-7 in the epidermis, *K5*-Cre mice and *Il7*-floxed mice[27] were each crossed to the $Rag2^{-/-}$ background ($Il7^{fl/fl}$;*K5*-Cre×$Rag2^{-/-}$ mice). $CD4^+$ T cells isolated from skin draining lymph nodes of DNFB-sensitized WT mice were transferred into $Il7^{fl/fl}$*K5*-Cre×$Rag2^{-/-}$ mice or control $Rag2^{-/-}$ mice. Recipient mice were challenged with DNFB 14 days after transfer and ear-swelling responses were assessed (Fig. 3d). Ear swelling and lymphocytic infiltration were reduced in $Il7^{fl/fl}$*K5*-Cre×$Rag2^{-/-}$ mice on days 2 and 3 after challenge (Fig. 3e,f). This transient effect might reflect the generation and influx of newly generated recipient T_{RM} after DNFB challenge.

A $CD4^+$ T cell lymphoma model with skin involvement

Epidermotropism of T cells is a histological hallmark of CTCL. In particular, lymphoma cells in mycosis fungoides exhibit a T_{RM} phenotype[18, 19,28]. *IL7* expression is increased in CTCL skin[29]. Whether lymphoma cells also require hair follicle-derived cytokines remains unclear. Thus, we extended our T_{RM} repopulation model in $Rag2^{-/-}$ mice by generating a novel lymphoma model.

Mutations in, or up regulation of, the oncogene *MYC*[30,31], as well as mutations in the tumor suppressor gene *INK4A/ARF* have been implicated in human lymphoma and CTCL[17,30]. $Ink4a/Arf^{-/-}$ mice are prone to tumor development including T cell lymphoma[32,33]. $Ink4a/Arf^{-/-}$ progenitor B cells transduced with *Myc* generate B cell lymphoma[34]. Taking advantage of these previous findings, we isolated $CD4^+$ T cells from $Ink4a/Arf^{-/-}$ mice and retrovirally transduced them with *Myc* (Fig. 4a). Approximately 50% of T cells were transduced, as determined by GFP expression ($Myc^+Ink4a/Arf^{-/-}$ $CD4^+$ T cells) (Fig. 4b). Recipient $Rag2^{-/-}$ mice developed erythroderma (redness and fine scaling of the entire skin surface) approximately three weeks after transfer of $Myc^+Ink4a/Arf^{-/-}$ $CD4^+$ T cells (Fig.

4c). Flow cytometry analysis revealed increased numbers of epidermotropic $CD4^+$ T cells (Fig. 4d), the majority of which expressed *Myc*-GFP (Fig. 4e) with increased IL-7Rα expression (Fig. 4e).

Histology revealed epidermotropism of lymphocytes with large, atypical nuclei, recapitulating that of human CTCL (Fig. 4f)[17]. Consistently, flow cytometry analysis revealed that *Myc*$^+$*Ink4a/Arf*$^{-/-}$ $CD4^+$ T cells were enlarged in size (Fig. 4g). Infiltrating lymphocytes expressed Ki-67, demonstrating that they were proliferative (Fig. 4h). Epidermotropic $CD4^+$ T cells were of the T_{RM} phenotype (Fig. 4i) and accumulated around the hair follicles (Fig. 4f,j). Collectively, *Myc*$^+$*Ink4a/Arf*$^{-/-}$ $CD4^+$ T cells transferred into *Rag2*$^{-/-}$ mice infiltrated skin and epidermis exhibiting histologic features of human CTCL. These mice also exhibited lymphoma in the lymph nodes and spleen, and died within 10 weeks after transfer (Supplementary Fig. 4), thereby also recapitulating an aspect of Sezary's syndrome, a leukemic subtype of CTCL[30].

Epidermotropism in CTCL depends on IL-7

To determine whether $CD4^+$ lymphoma cells also relied on hair follicle-derived IL-7, we transferred *Myc*$^+$*Ink4a/Arf*$^{-/-}$ $CD4^+$ T cells into *Rag2*$^{-/-}$ or *Il7*$^{fl/fl}$*K5*-Cre×*Rag2*$^{-/-}$ mice (Fig. 5a). In contrast to *Rag2*$^{-/-}$ mice, *Il7*$^{fl/fl}$*K5*-Cre×*Rag2*$^{-/-}$ mice did not develop erythroderma (Fig. 5b). Furthermore, the absolute numbers of epidermotropic lymphoma cells were reduced in the absence of hair follicle-derived IL-7 (Fig. 5c), whereas significant differences were not observed in the spleen and lymph nodes (Fig. 5d). Histologic analysis of control *Rag2*$^{-/-}$ mice revealed abundant epidermotropic lymphocytes with epidermal thickening, but histological changes were minimal in *Il7*$^{fl/fl}$*K5*-Cre×*Rag2*$^{-/-}$ mice (Fig. 5e). Visualization of $CD4^+$ T cells in epidermal sheets confirmed these findings (Fig. 5f). Thus, epidermotropic $CD4^+$ T_{RM} require continued hair follicle-derived IL-7 after neoplastic transformation.

In CTCL, IL-7 is upregulated in human hair follicles

To examine if our findings could be extended to humans, we studied human hair follicles. Whereas hair follicles in the trunk skin of mice and humans are mostly in telogen, the majority of those in human scalp are in anagen. The terminus end is called the bulb, and the portion between the bulb and the stem cell-containing bulge is referred to as the suprabulb (Fig. 6a and Supplementary Fig. 5). We dissected hair follicles from normal human scalp into interfollicular epidermis, infundibulum, bulge, suprabulb and bulb, and obtained RNA from each of these sites (Fig. 6a)[4] and performed real-time PCR for *IL15* and *IL7*. *IL15* was predominantly expressed by hair follicle keratinocytes in the suprabulb, and *IL7* expression was highest in the infundibulum and suprabulb (Fig. 6b).

We additionally evaluated IL-7 expression in hair follicles from normal human scalp and lesional scalp skin of patients with CTCL. Faint staining for IL-7 was detected in normal human hair follicles via immunohistochemistry. IL-7 expression was apparent in a CTCL subject, in which the staining was detected in the infundibulum and the suprabulbar area (Fig. 6c), consistent with the real-time PCR data from normal human scalp. In other patients,

IL-7 staining was increased not only in hair follicle keratinocytes, but also in keratinocytes in the interfollicular epidermis (Supplementary Fig. 6).

Consistent with our observations in mice, IL-7R expression by T cells was increased in lesional CTCL epidermis in comparison to that on T cells in normal human scalp skin (Fig. 6d and Supplementary Fig. 5). IL-7R expression in lesional keratinocytes in CTCL appears to be increased, although the significance of this has yet to be determined.

Discussion

Epidermotropism of T_{RM}, both non-malignant and malignant, is supported by the hair follicle-derived cytokines IL-7 and IL-15. Previous studies have focused on T_{RM} biology in the context of viral infections. We studied the requirement of epidermotropic T_{RM} during steady state by utilizing non-malignant and malignant models. The lack of hair follicle-derived cytokines led to the failure of both $CD4^+$ and $CD8^+$ T_{RM} to persist in skin. Impaired CHS responses in the absence of hair follicle-derived cytokines highlight the importance of homeostatic organization of T_{RM} prior to inflammation.

The requirement of IL-7 and IL-15 in the generation and maintenance of memory T cells is well-established[24,25], but the fate of T_{RM} in peripheral tissues that are deprived of these cytokines remains unclear. In particular, whether the cells undergo cell death or migration deserves further attention in the context of lymphoma.

The tropism that $CD4^+$ T_{RM} exhibit to the hair follicles demonstrated in this study is compatible and complementary to a previous report in which approximately 30% of virus-specific $CD4^+$ memory T cells were found to associate with the hair follicles after herpes simplex virus skin infection[7]. To date, T_{RM} in the skin has mainly been characterized in the context of $CD8^+$ T cells. Although $CD4^+$ memory T cells may well be comparable to $CD8^+$ T_{RM} as skin residents based on surface marker expression and past reports[13,22], thorough studies on $CD4^+$ memory T cells as *bona fide* T_{RM} has yet to be performed. Our observation that epidermal and dermal T_{RM} have subtle differences in CD103 expression and the higher ratio of $CD4^+$ $FoxP3^+$ T_{RM} in the dermis suggests that $CD4^+$ T_{RM} in these skin compartments might be regulated via distinct mechanisms.

In conclusion, we have demonstrated the importance of hair follicle-derived IL-7 and IL-15 in T_{RM} homeostasis in the epidermis which represent attractive therapeutic targets in inflammatory skin diseases and malignant lymphoma, the concept of which may also be relevant in other peripheral tissues.

ONLINE METHODS

Mice

C57 BL/6J (CD45.2) mice and *Il15*$^{-/-}$ mice were purchased from CLEA Japan. C57 BL/6J *Rag2*$^{-/-}$ mice were purchased from the Central Institute for Experimental Animals (Tokyo, Japan). *K14*-Cre^{ERT} mice were purchased from Jackson Laboratory (ME, U.S.A.)[26]. *Ink4a/Arf*$^{-/-}$ mice (B6.129-Cdkn2atm1Rdp) were from Mouse Models of Human Cancers Consortium (NCI-Frederick)[33]. *Il7*-floxed mice, *K5*-Cre mice (kindly provided by Junji

Takeda, Osaka University), Langerin-DTA mice and Langerin-DTR mice (kindly provided by Daniel H. Kaplan, University of Minnesota and Björn E. Clausen, Johannes Gutenberg University of Mainz, respectively) were generated as previously described[27,35–37]. Only female mice 6 to 12 weeks of age were used for experiments. All mice were bred and housed in a specific pathogen-free condition. All animal procedures and study protocols were approved by the Keio University Ethics Committee for Animal Experiments.

Human tissue

All samples for this study were obtained according to protocols approved by the Institutional Review Board of Keio University (protocol number 2003-0057) or NCI, NIH (protocol number 96-C-0102). Informed consent was obtained from all subjects prior to the acquisition of the skin tissues. Two sets of normal human scalp samples for gene analysis and formalin-fixed scalp samples for histopathological examination were obtained from excess normal skin that resulted from surgical removal of benign, subcutaneous skin tumors. Formalin-fixed scalp samples from subjects with CTCL were biopsy specimen obtained from lesional skin for diagnosis.

Preparation of epidermal sheets

Epidermal sheets were prepared as before[4] with slight modification. Briefly, ears were split into dorsal and ventral halves with forceps. Thioglycolic acid-containing Hair Removing Body Cream Epilat (Kracie) was used to remove hair in some experiments. Ear halves were incubated for 15 minutes at 37°C on 3.8% ammonium thiocyanate (Wako Pure Chemical Industries) in phosphate buffer (pH 7.0). Epidermal sheets were manually detached from the dermis under a dissecting microscope (Olympus).

Preparation of epidermal and dermal cell suspensions

Epidermal and dermal cell suspensions were prepared as before[4] with slight modification. Briefly, shaved whole trunk skin was harvested from appropriate animals and, after removal of subcutaneous tissues with forceps, was floated with epidermal side up onto 10 mL of Trypsin-EDTA solution containing 5 mL of 0.25% Trypsin (Nacalai tesque) and 5 mL of 0.05% Trypsin-0.53 mM EDTA • 4Na (Nacalai tesque) at 37°C for less than 30 minutes in 10 cm dish. Epidermis and dermis were separated manually with forceps. Dermis was cut into small chips manually with scissors and further incubated in 4 mL of RPMI containing 0.03% Liberase TL Research grade (Roche Applied Science) and 200 U/mL of DNase (Wako Pure Chemical Industries) for 60 minutes at 37°C shaking with rotation at 200 rpm (Bioshaker, Taitec). Epidermal and dermal cells were then suspended in 5% FCS in PBS, washed and filtered through Cell strainer (BD Falcon).

Antibodies for immunofluorescence microscopy and flow cytometry analysis for mouse samples

Anti-mouse CD4 monoclonal antibody (clone GK1.5, BioLegend) was used in conjugated forms pre-labeled with PE/Cy7 or APC or labeled in house with Alexa Fluor 568 (Invitrogen). Anti-mouse CD8 monoclonal antibody (clone 53.6.7, BioLegend) was used in conjugated forms pre-labeled with FITC, APC, APC/Cy7 or AmCyan or labeled in house

with Alexa Fluor 647 (Invitrogen). The following pre-labeled monoclonal antibodies and polyclonal antibodies, all obtained from BioLegend unless otherwise stated, were used for immunofluorescence microspcopy and flow cytometry: CD3ε (clone 145-2c11), TCRγδ (clone GL3), MHC II (anti-IA/IE; clone M5/114.15.2), CD34 (clone RAM34, eBioscience), CD44 (clone IMF7), CD45 (clone 30F-11), CD49f (anti-integrinα_6; clone GoH3), CD62L (clone MEL-14), CD69 (clone H1.2F3), CD103 (clone 2E7), CD122 (anti-IL-15/2Rβ; clone 5H4), CD127 (anti-IL-7Rα; clone SB/199), EpCAM (clone G8.8), Ly-6A/E (anti-Sca-1; clone E13-161.7), Antibodies that were labeled in-house were stored at 0.5mg/ml concentration. All primary antibodies for flow cytometry were diluted 1:200 with the exception of clone G8.8, which was used at 1:800 dilution. For immunofluorescence microscopy, primary antibodies were used at 1:100 dilution.

Primary antibodies were detected, if needed, with Alexa Fluor labeled secondary antibodies (anti-Fluorescein/Oregon Green, A11096 or anti-Green Fluorescent Protein, A21311; both from Life Technologies) at 1:200 dilution. Anti-mouse CD16/32 (clone 93, BioLegend) was routinely used (1:100 dilution) to block Fcγ receptors prior to staining.

Immunofluorescence microscopy

Staining of epidermal sheets and frozen skin sections was performed as before[4] with slight modification. Briefly, sheets and sections were fixed in acetone for 5 minutes at −20°C or in 4% paraformaldehyde (Wako Pure Chemical Industries) in PBS for 15 minutes at room temperature, and were rehydrated or washed in PBS for 5 minutes. They were blocked in 3% dry milk (Morinaga) in PBS with 5% goat serum for at least an hour at room temperature. For intracellular staining, 0.2% Triton X-100 (Sigma-Aldrich) was added in blocking buffer. Primary antibodies were diluted in blocking buffer and incubated overnight at 4°C. After washing, primary antibodies were detected with appropriate secondary antibodies and nuclei were visualized with Hoechst 33258 (Invitrogen). Mouse lips were routinely used for vertical sections because this provided wide view of vertical and horizontal sections of both pelage hair and vibrissae. Images were mostly observed with Zeiss Axio Observer. Z1 with or without Apotome (Carl Zeiss), collected with the Axiovision software (ver. 4.8). Adjustments of levels, if needed, were performed on Photoshop CS 5.1 (Adobe), where controls were also treated identically.

Flow cytometry analysis and cell sorting

Data were collected utilizing FACS Canto II (BD Biosciences) and analyzed with Flow Jo (Tree star). Non-viable cells were omitted using propidium iodide (Sigma-Aldrich) staining or Live/Dead cell (Invitrogen) pre-staining for fixed and permeabilized cells before primary antibody staining. Fluorescence activated cell sorting of hair follicle keratinocyte subsets was performed with FACSAria II (BD Biosciences) or MoFlow (Beckman Coulter), during which cells were directly sorted into TRIzol LS (Invitrogen) and divided into five subsets based on the expression of cell-surface markers as described before[4]; interfollicular epidermis (MHCII$^-$CD45$^-$Sca-1$^+$ EpCAM^{low}), infundibulum (MHCII$^-$CD45$^-$Sca-1$^+$ EpCAM^{int}), isthmus (MHCII$^-$CD45$^-$Sca-1$^-$EpCAM^{hi}), basal bulge (MHCII$^-$CD45$^-$Sca-1$^-$CD34$^+$ integrin α_6^+) or suprabasal layer bulge

(MHCII$^-$CD45$^-$Sca-1$^-$CD34$^+$ integrin α_6^-). Sorted cells were further processed for RNA extraction.

Isolation of human hair follicles for gene analysis

Samples taken from human scalp were dissected as previously described[4]. Briefly, scalp samples were dissected into five anatomical areas (interfollicular epidermis, infundibulum, bulge, suprabulb and bulb) under a dissecting microscope, and were then incubated overnight at 4°C with 1,500 U/mL of Dispase II (Godo Syusei) in DMEM to remove non-epidermal components.

Real-time PCR

Cytokine expressions of hair follicle keratinocyte subsets were analyzed as previously described[4]. Briefly, total mRNA was purified from FACS-sorted epidermal keratinocyte population, using an RNeasy Micro Kit (QIAGEN). cDNA was synthesized using SuperScript III First-Strand Synthesis SuperMix for qRT-PCR (Invitrogen), and then real-time PCR analysis was performed using Power SYBR Green PCR Master Mix (Applied Biosystems) and StepOne Real-Time PCR system (Applied Biosystems), according to the manufacturer's protocol. All primers (Supplementary Table 1) were designed using Primer Express software (Applied Biosystems) and reactions were conducted under the following cycling conditions: 10 minutes at 95°C followed by 40 cycles of 15 seconds at 95°C and 60 seconds at 60°C. Normalization of mRNA expression was performed based on the expression of β-Actin utilizing cycling threshold (ΔC_T) method and the amount of PCR product was calculated based on $2^{-\Delta CT}$ (ref. 38). Results were presented as ± standard deviations.

T_{RM} repopulation model

Spleens from 8-week-old C57BL/6J mice were harvested and homogenized on sterile silicone meshes and were then filtered through Cell Strainer (BD Falcon). Cells were washed in 5% FCS in PBS, centrifuged, and resuspended in PBS to obtain whole splenocyte single cell suspension. 5×10^6 splenocytes in 200 μl PBS were adoptively transferred i.v. into 6 to 10-week-old lymphopenic recipients.

Generation of bone marrow chimeras

C57BL/6J WT or *Il15*$^{-/-}$ mice were lethally irradiated (950 rad) and were transferred i.v. with 2×10^6 total bone marrow cells from *Rag2*$^{-/-}$ mice on the following day to generate lymphopenic bone marrow chimeric mice (WT^{Rag} or *Il15* KO^{Rag}), which were then used as recipients in T_{RM} repopulation experiments.

FTY720 and tamoxifen treatment

Il7$^{fl/fl}$*K14*-Cre^{ERT} or *Il7*$^{fl/wt}$*K14*-Cre^{ERT} mice were injected i.p. with 1 mg of tamoxifen (Cayman) in 100 μL of sunflower oil (Nacalai tesque)/day for 5 consecutive days (day 0 to 4)[39]. 30 μg of FTY720 (Cayman) was injected i.p. from day -1 for 7 consecutive days[8] and every other day thereafter, until tissues were harvested.

FTY720 and diphtheria toxin (DT) treatment

For *in vivo* depletion of LCs, Langerin-DTR mice (or control WT mice) were injected i.p. with 500 ng of DT[40] (Sigma, USA) in 200 μL of sterile PBS at days 0 and 7. 30 μg of FTY720 (Cayman) was injected i.p. from day -1 for 7 consecutive days and every other day thereafter, until tissues were harvested.

Hapten-induced contact hypersensitivity

WT donor mice were sensitized as described[41] with slight modification. Briefly, 60 μL of 0.5% 1-fluoro-2,4-dinitrobenzene (DNFB) in vehicle (olive oil: acetone = 1:4) or vehicle alone was topically applied to the shaved-trunk skin, ears and paws of WT mice. 5 days after sensitization, 1×10^6 $CD4^+$ or $CD8^+$ T cells, which were purified via MACS cell separation system (Miltenyi Biotec) from skin-draining lymph nodes, were adoptively transferred into lymphopenic recipients. 2 weeks after transfer, the ears were challenged with 10 μL of 0.3% DNFB. Ear swelling, (ear thickness on day x) − (basal ear thickness on day 0), was measured in a blinded fashion by an investigator that was not involved in the study.

T cell lymphoma model with skin involvement

Mouse c-*Myc* was cloned into the retroviral vector pMXs-IG, which was transfected and transduced as described with slight modification[34,42]. Briefly, the pMX-based vector (*Myc*-GFP) was transfected into a packaging cell line, Plat-E[43], using FuGENE HD Transfection Reagent (Roche Applied Science) and then the viral supernatant was collected after 48 hours of incubation. $CD4^+$ T cells, which were collected and enriched from spleen and skin-draining lymph nodes of *Ink4a/Arf*$^{-/-}$ mice by positive selection utilizing the MACS cell separation system, were cultured in complete medium (RPMI 1640 containing 10% FCS, 2 mM L-glutamine, 1 mM pyruvate, 50 U/mL penicillin, 50 μg/mL streptomycin, 0.05 mM 2-ME) supplemented with 100 U/mL hIL-2 and 2.5μg/mL Con A at 37°C for 24 hours. Flow through cells that were collected after $CD4^+$ T cell enrichment were irradiated (3,000 rad) and used as feeder cells for co-culture with $CD4^+$ T cells. The activated $CD4^+$ T cells were then resuspended in retroviral supernatant and centrifuged (3,000 rpm, 1 hour, 30°C). After incubation at 37°C for four hours, the retroviral supernatant was removed, and the cells were further cultured in complete medium supplemented with 100 U/mL hIL-2 at 37°C for 44 hours. The whole bulk of cultured T cells were transferred i.v. into *Rag2*$^{-/-}$ or *Il7*$^{fl/fl}$*K5*-Cre×*Rag2*$^{-/-}$ mice. To avoid inter-experimental variability due to subtle differences in transduction efficiency, the number of transferred cells was normalized to contain 2.5×10^5 *Myc*-GFP^+ $CD4^+$ cells. Equivalent numbers of $CD4^+$ T cells from WT splenocytes were transferred i.v. into *Rag2*$^{-/-}$ mice. To address the contribution of hair follicle-derived IL-7, the bulk of transduced T cells, numbers normalized as above, were transferred into *Rag2*$^{-/-}$ or *Il7*$^{fl/fl}$*K5*-Cre×*Rag2*$^{-/-}$ mice.

Preparation of transverse sections

4-mm punch biopsy specimens were sliced at four levels[44]; just beneath the epidermis (infundibulum), sebaceous glands attachment (bulge), between sebaceous glands attachment and bulb (suprabulb), and bulb. Tissues were sectioned and a single slide containing 5μm-

disks from four different layers were analyzed for histology or immunohistochemistry (Supplementary Fig. 4).

Histopathological and immunohistochemical analysis of human and mouse skin sections

Tissues were fixed in 10% neutral buffered formalin, embedded in paraffin, and sectioned at a thickness of 5 μm. Sections were paraffin-depleted and rehydrated in a graded series of ethanol solutions. For histology, sections were stained with hematoxylin and eosin. For immunohistochemistry staining for human IL-7 expression, sections were washed with PBS and treated with 3% H_2O_2, before incubation with the following primary antibody: rabbit anti-IL-7 polyclonal antibody (clone sc-7921, Santa Cruz Biotechnology) (1:100). For IL-7R expression, sections were autoclaved at 120°C for 1 minute in 5 mM EDTA buffer (pH 8.0) and were allowed to cool at room temperature before incubation with the following primary antibody: rabbit anti-IL-7R polyclonal antibody (clone sc-25475, Santa Cruz Biotechnology) (1:100). Immune complexes were detected by using the ImmPRESS REAGENT KIT (Vector Laboratories) with 3, 3'-diaminobenzidine, and sections were counterstained with hematoxylin. For immunohistochemistry of mouse samples for Ki-67 expression, sections were subjected to 20 minutes microwave treatment in citrate buffer (pH 7.0) and were allowed to cool at room temperature. Non-specific binding was blocked in 3% dry milk PBS with 5% goat serum for 1 hour at room temperature, before incubation with the following primary antibody: rabbit anti-Ki67 monoclonal antibody (clone SP6, Thermo Scientific Lab Vision) (1:100), and then washed, and bound antibodies were detected with Histofine Simple Stain MAX PO (Nichirei Corporation). Secondary antibodies were further visualized with ImmPACT DAB (Vector Laboratories), and sections were counterstained with hematoxylin. Images were collected via an inverted microscope (BX41, Olympus), equipped with a digital camera (DP20, Olympus).

Statistics

Statistical significance was calculated with an unpaired two-tailed Student's *t* test or a two-way ANOVA using GraphPad Prism 6 (GraphPad software). The values presented are expressed as the means +/− standard error of the mean (s.e.m.). Variances were similar between groups in all experiments as determined by the *F* test using GraphPad Prism 6. For all statistical analyses, data were considered significant when $P \leq 0.05$ (*), $P \leq 0.01$ (**) or $P \leq 0.001$ (***). The animal experiments were not randomized. The investigators were not blinded to allocation during experiments and analyses unless otherwise indicated.

Supplementary Material

Refer to Web version on PubMed Central for supplementary material.

ACKNOWLEDGMENTS

We thank Manabu Ohyama for helpful discussion on human hair follicles, N. Sakai, K. Eguchi, and S. Sato for assistance (Department of Dermatology, Keio University School of Medicine), Heidi H. Kong (Dermatology Branch, CCR, NCI, NIH) on human CTCL, Y. Madokoro (Department of Pathology, Keio University School of Medicine) for human CTCL immunohistochemical staining, T. Kitamura (The University of Tokyo) for providing the retroviral vector pMXs-IG and Plat-E cells. This work was supported by the Japan Society for the Promotion of Science, The Kanae Foundation for the Promotion of Medical Science, JSID's Fellowship Shiseido Award, and the U.S. National Institutes of Health (NIH) NCI Intramural Research Programs.

REFERENCES

1. Cotsarelis G, Sun TT, Lavker RM. Label-retaining cells reside in the bulge area of pilosebaceous unit: implications for follicular stem cells, hair cycle, and skin carcinogenesis. Cell. 1990; 61:1329–1337. [PubMed: 2364430]
2. Nishimura EK, et al. Dominant role of the niche in melanocyte stem-cell fate determination. Nature. 2002; 416:854–860. [PubMed: 11976685]
3. Christoph T, et al. The human hair follicle immune system: cellular composition and immune privilege. Br J Dermatol. 2000; 142:862–873. [PubMed: 10809841]
4. Nagao K, et al. Stress-induced production of chemokines by hair follicles regulates the trafficking of dendritic cells in skin. Nat Immunol. 2012; 13:744–752. [PubMed: 22729248]
5. Clark RA, et al. The vast majority of CLA+ T cells are resident in normal skin. J Immunol. 2006; 176:4431–4439. [PubMed: 16547281]
6. Gebhardt T, et al. Memory T cells in nonlymphoid tissue that provide enhanced local immunity during infection with herpes simplex virus. Nat Immunol. 2009; 10:524–530. [PubMed: 19305395]
7. Gebhardt T, et al. Different patterns of peripheral migration by memory CD4+ and CD8+ T cells. Nature. 2011; 477:216–219. [PubMed: 21841802]
8. Jiang X, et al. Skin infection generates non-migratory memory CD8+ T(RM) cells providing global skin immunity. Nature. 2012; 483:227–231. [PubMed: 22388819]
9. Wakim LM, Waithman J, van Rooijen N, Heath WR, Carbone FR. Dendritic cell-induced memory T cell activation in nonlymphoid tissues. Science. 2008; 319:198–202. [PubMed: 18187654]
10. Mackay LK, et al. The developmental pathway for CD103(+)CD8+ tissue-resident memory T cells of skin. Nat Immunol. 2013; 14:1294–1301. [PubMed: 24162776]
11. Shiow LR, et al. CD69 acts downstream of interferon-[alpha]/[beta] to inhibit S1P1 and lymphocyte egress from lymphoid organs. Nature. 2006; 440:540–544. [PubMed: 16525420]
12. Bromley SK, Yan S, Tomura M, Kanagawa O, Luster AD. Recirculating Memory T Cells Are a Unique Subset of CD4+ T Cells with a Distinct Phenotype and Migratory Pattern. J Immunol. 2013; 190:970–976. [PubMed: 23255361]
13. Suffia I, Reckling SK, Salay G, Belkaid Y. A Role for CD103 in the Retention of CD4+CD25+ Treg and Control of Leishmania major Infection. J Immunol. 2005; 174:5444–5455. [PubMed: 15845457]
14. Sanchez Rodriguez R, et al. Memory regulatory T cells reside in human skin. J Clin Invest. 2014; 124:1027–1036. [PubMed: 24509084]
15. Shiohara T, Moriya N. Epidermal T cells: their functional role and disease relevance for dermatologists. J Invest Dermatol. 1997; 109:271–275. [PubMed: 9284089]
16. Mizukawa Y, et al. Direct evidence for interferon-gamma production by effector-memory-type intraepidermal T cells residing at an effector site of immunopathology in fixed drug eruption. Am J Pathol. 2002; 161:1337–1347. [PubMed: 12368207]
17. Hwang ST, Janik JE, Jaffe ES, Wilson WH. Mycosis fungoides and Sezary syndrome. Lancet. 2008; 371:945–957. [PubMed: 18342689]
18. Campbell JJ, Clark RA, Watanabe R, Kupper TS. Sezary syndrome and mycosis fungoides arise from distinct T-cell subsets: a biologic rationale for their distinct clinical behaviors. Blood. 2010; 116:767–771. [PubMed: 20484084]
19. Clark RA, et al. Skin effector memory T cells do not recirculate and provide immune protection in alemtuzumab-treated CTCL patients. Sci Transl Med. 2012; 4:117ra117.
20. Edelson RL. Cutaneous T cell lymphoma: mycosis fungoides, Sezary syndrome, and other variants. J Am Acad Dermatol. 1980; 2:89–106. [PubMed: 6988470]
21. Seneschal J, Clark RA, Gehad A, Baecher-Allan CM, Kupper TS. Human epidermal Langerhans cells maintain immune homeostasis in skin by activating skin resident regulatory T cells. Immunity. 2012; 36:873–884. [PubMed: 22560445]
22. Sanchez Rodriguez R, et al. Memory regulatory T cells reside in human skin. J Clin Invest. 2014; 124:1027–1036. [PubMed: 24509084]

23. Ariotti S, et al. T cell memory. Skin-resident memory CD8(+) T cells trigger a state of tissue-wide pathogen alert. Science. 2014; 346:101–105. [PubMed: 25278612]
24. Lanzavecchia A, Sallusto F. Understanding the generation and function of memory T cell subsets. Curr Opin Immunol. 2005; 17:326–332. [PubMed: 15886125]
25. van Leeuwen EM, Sprent J, Surh CD. Generation and maintenance of memory CD4(+) T Cells. Curr Opin Immunol. 2009; 21:167–172. [PubMed: 19282163]
26. Vasioukhin V, Degenstein L, Wise B, Fuchs E. The magical touch: genome targeting in epidermal stem cells induced by tamoxifen application to mouse skin. Proc Natl Acad Sci U S A. 1999; 96:8551–8556. [PubMed: 10411913]
27. Liang B, et al. Role of hepatocyte-derived IL-7 in maintenance of intrahepatic NKT cells and T cells and development of B cells in fetal liver. J Immunol. 2012; 189:4444–4450. [PubMed: 23018454]
28. Dorfman DM, Shahsafaei A. CD69 expression correlates with expression of other markers of Th1 T cell differentiation in peripheral T cell lymphomas. Hum Pathol. 2002; 33:330–334. [PubMed: 11979374]
29. Yamanaka K, et al. Skin-derived interleukin-7 contributes to the proliferation of lymphocytes in cutaneous T-cell lymphoma. Blood. 2006; 107:2440–2445. [PubMed: 16322477]
30. Espinet B, Salgado R. Mycosis fungoides and Sezary syndrome. Methods Mol Biol. 2013; 973:175–188. [PubMed: 23412790]
31. Kanavaros P, et al. Mycosis fungoides: expression of C-myc p62 p53, bcl-2 and PCNA proteins and absence of association with Epstein-Barr virus. Pathol Res Pract. 1994; 190:767–774. [PubMed: 7831152]
32. Kamijo T, Bodner S, van de Kamp E, Randle DH, Sherr CJ. Tumor spectrum in ARF-deficient mice. Cancer Res. 1999; 59:2217–2222. [PubMed: 10232611]
33. Serrano M, et al. Role of the INK4a locus in tumor suppression and cell mortality. Cell. 1996; 85:27–37. [PubMed: 8620534]
34. Sugihara E, et al. Ink4a and Arf are crucial factors in the determination of the cell of origin and the therapeutic sensitivity of Myc-induced mouse lymphoid tumor. Oncogene. 2012; 31:2849–2861. [PubMed: 21986948]

REFERENCES

35. Tarutani M, et al. Tissue-specific knockout of the mouse Pig-a gene reveals important roles for GPI-anchored proteins in skin development. Proc Natl Acad Sci U S A. 1997; 94:7400–7405. [PubMed: 9207103]
36. Kaplan DH, Jenison MC, Saeland S, Shlomchik WD, Shlomchik MJ. Epidermal langerhans cell-deficient mice develop enhanced contact hypersensitivity. Immunity. 2005; 23:611–620. [PubMed: 16356859]
37. Bennett CL, et al. Inducible ablation of mouse Langerhans cells diminishes but fails to abrogate contact hypersensitivity. J Cell Biol. 2005; 169:569–576. [PubMed: 15897263]
38. Livak KK, Schmittgen TD. Analysis of relative gene expression data using real-time quantitative PCR and the 2 (−delta delta C(T)) method. Methods. 2001; 25:402–408. [PubMed: 11846609]
39. Li M, et al. Skin abnormalities generated by temporally controlled RXRalpha mutations in mouse epidermis. Nature. 2000; 407:633–636. [PubMed: 11034212]
40. Ouchi T, et al. Langerhans cell antigen capture through tight junctions confers preemptive immunity in experimental staphylococcal scalded skin syndrome. J Exp Med. 2011; 208:2607–2613. [PubMed: 22143886]
41. Fyhrquist N, Wolff H, Lauerma A, Alenius H. CD8+ T cell migration to the skin requires CD4+ help in a murine model of contact hypersensitivity. PLoS One. 2012; 7:e41038. [PubMed: 22916101]
42. Takahashi H, et al. Desmoglein 3-specific CD4+ T cells induce pemphigus vulgaris and interface dermatitis in mice. J Clin Invest. 2011; 121:3677–3688. [PubMed: 21821914]
43. Morita S, Kojima T, Kitamura T. Plat-E: an efficient and stable system for transient packaging of retroviruses. Gene Ther. 2000; 7:1063–1066. [PubMed: 10871756]

44. Evaluating and Describing Transverse (Horizontal) Sections. An Atlas of Hair Pathology with Clinical Correlations. :17–25.

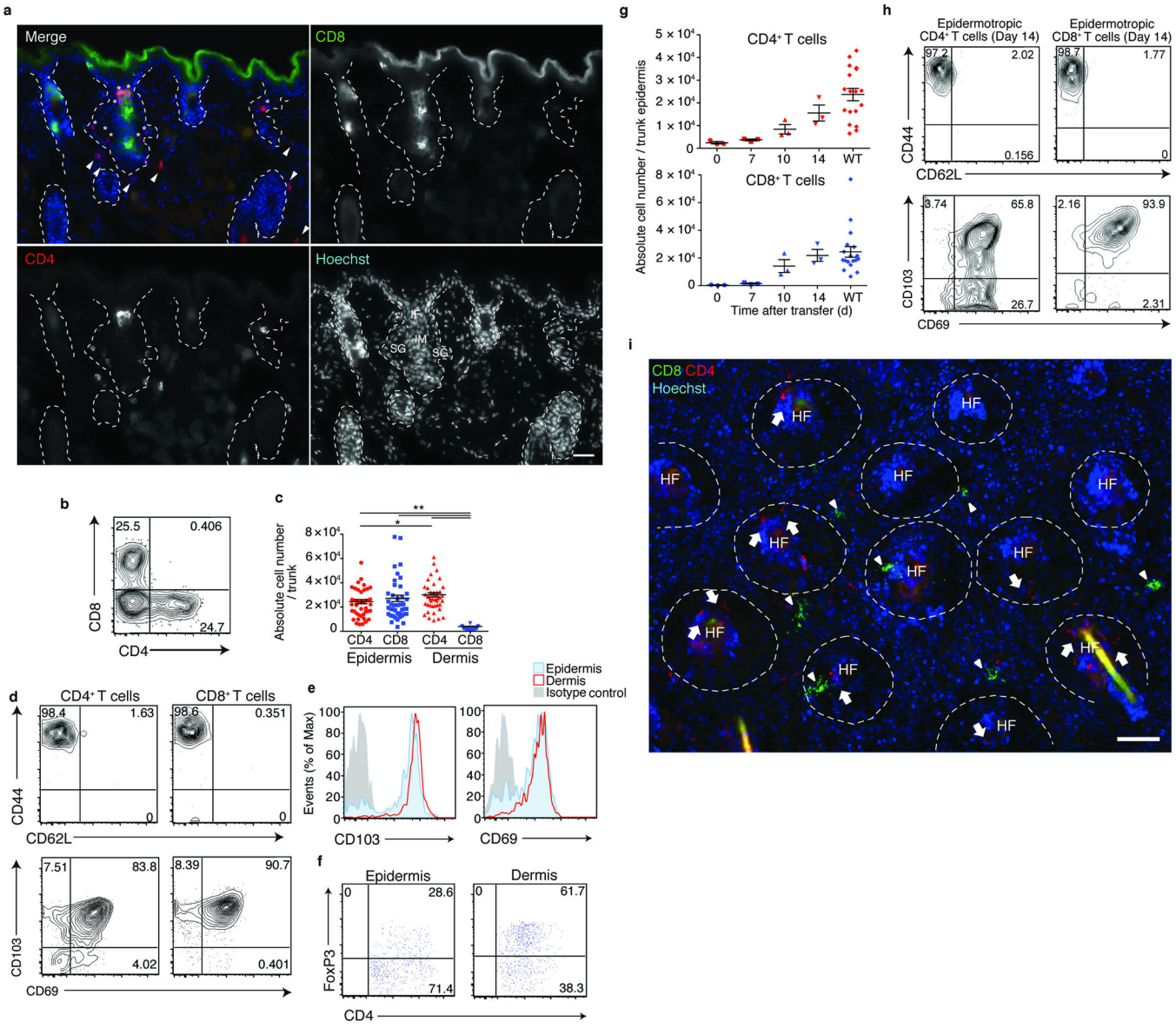

Figure 1. Epidermotropic CD4$^+$ and CD8$^+$ T_{RM} associate with hair follicles

(a) Skin sections from WT mice, stained as indicated. Dotted lines delineate hair follicles. Asterisk and arrowheads depict CD4$^+$ T cells in epidermis and dermis, respectively. Scale bar, 50 μm. **(b)** Flow cytometry analysis of CD45$^+$CD3$^+$MHCII$^-$TCRγδ$^-$ epidermal cells from WT mice. Numbers in quadrants represent percentage among the gated subset **(c)** T cell numbers in the epidermis and dermis. Each symbol represents individual mice; horizontal lines depict the mean and error bars indicate s.e.m. *P < 0.05, **P < 0.01 (unpaired two-tailed Student's *t*-test). **(d)** CD44 and CD62L, and CD103 and CD69 expression on T cells in the epidermis. **(e)** Expression of CD103 and CD69 expression on CD4$^+$ T cells in the epidermis (red) and dermis (blue) with isotype controls (grey). (**f**) Frequency of CD4$^+$FoxP3$^+$ T_{reg} cells in the epidermis and dermis. **(g)** Number of donor T cells in *Rag2*$^{-/-}$ recipient epidermis monitored via flow cytometry at indicated dates after adoptive transfer of WT splenocytes. **(h)** Epidermotropic T cells from (**g**) were analyzed via

flow cytometry as in (**d**), 14 d after transfer. Shown are $CD45^+CD3^+MHCII^-TCR\gamma\delta^-$ $CD4^+$ (left panels) or $CD8^+$ (right panels) populations. **(i)** Epidermal sheets from mice as in (**g**), day 14 after transfer, were stained as indicated. Dashed lines delineate hair follicles. Scale bar, 100 μm. Data are from one experiment representative of three independent experiments with three mice per group (a,b,d–k) or from ten independent experiments with a total of 42 mice (**c**).

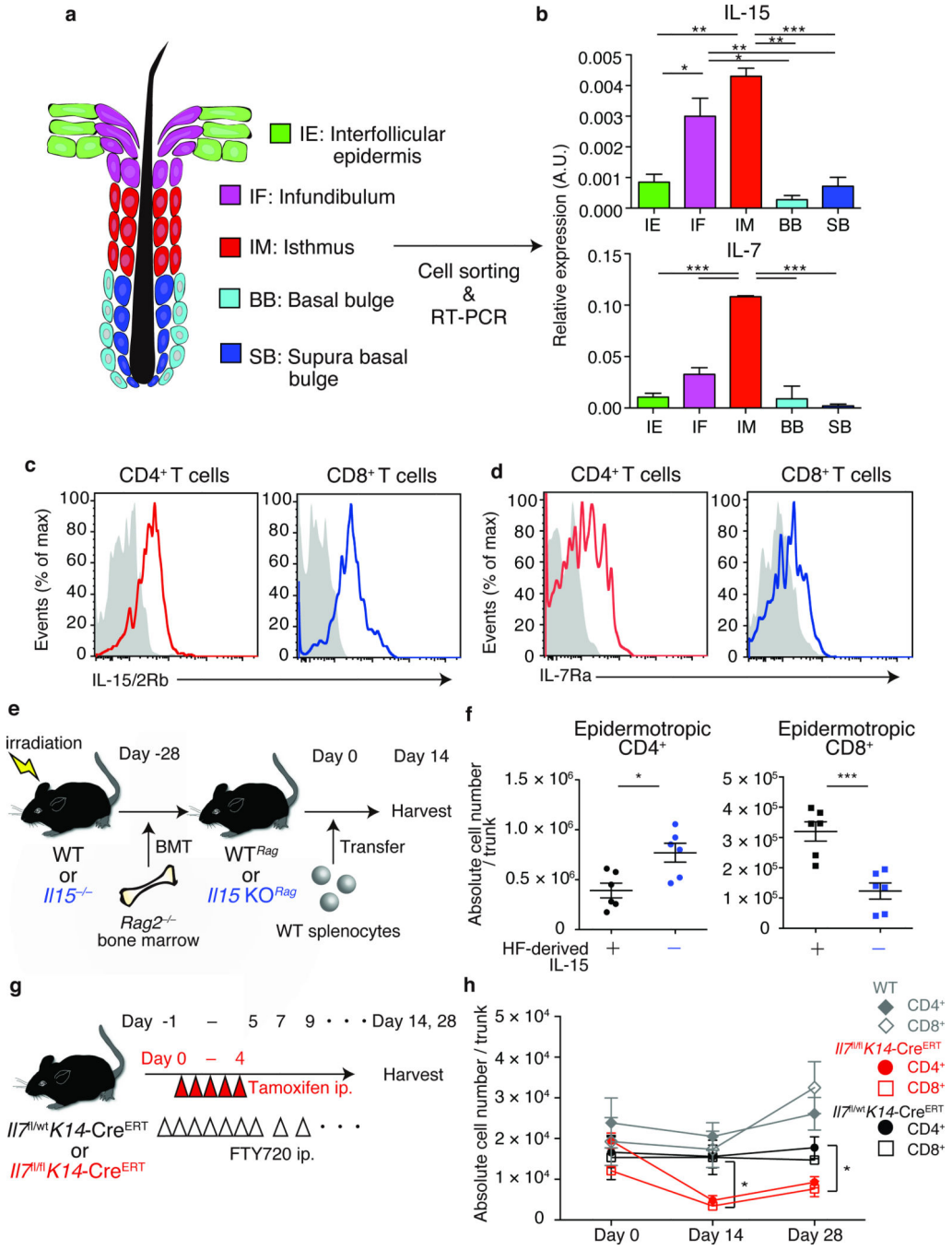

Figure 2. Epidermotropic T_{RM} require hair follicle-derived cytokines

(**a**) Schematic representation of mouse hair follicle keratinocytes in telogen. Keratinocytes were sorted into five subsets based on cell-surface marker expressions. (**b**) Real-time PCR analysis for *il15* and *il7* expressions by hair follicle keratinocyte subsets, presented in arbitrary units (A.U.), relative to *Actb* expression. (**c**) IL-15/2 receptor β (IL-15/2Rβ) and (**d**) IL-7 receptor α (IL-7Rα) expression by T_{RM}, assessed via flow cytometry, gated on the $CD45^+CD3^+MHCII^-TCR\gamma\delta^-$ population ($n = 3$). (**e**) Experimental scheme for the analysis of T_{RM} dependence on hair follicle-derived IL-15. WT or *il15*$^{-/-}$ mice were reconstituted

with *Rag2*$^{-/-}$ bone marrow (WT^{Rag} or *Il15* KO^{Rag}), and were transferred with WT splenocytes. (**f**) Epidermotropic T_{RM} numbers in recipient WT^{Rag} or *il15* KO^{Rag} mice (n = 6). Symbols represent individual mice. (**g**) Experimental scheme for analyzing T_{RM} dependence on hair follicle-derived IL-7. Indicated mice were treated with tamoxifen i.p. on days 0 to 4. FTY720 was injected i.p. from day -1 for 7 consecutive days and every other day thereafter, until tissue harvest. (**h**) **E**pidermotropic T_{RM} numbers after tamoxifen-induced ablation of hair follicle IL-7 (n = 3). Data are representative of three (**b–d**) or two (**f, h**) independent experiments. *P < 0.05, **P < 0.01, ***P < 0.001 (unpaired two-tailed Student's *t*-test). Horizontal lines depict the mean, and error bars indicate s.e.m. in all graphs.

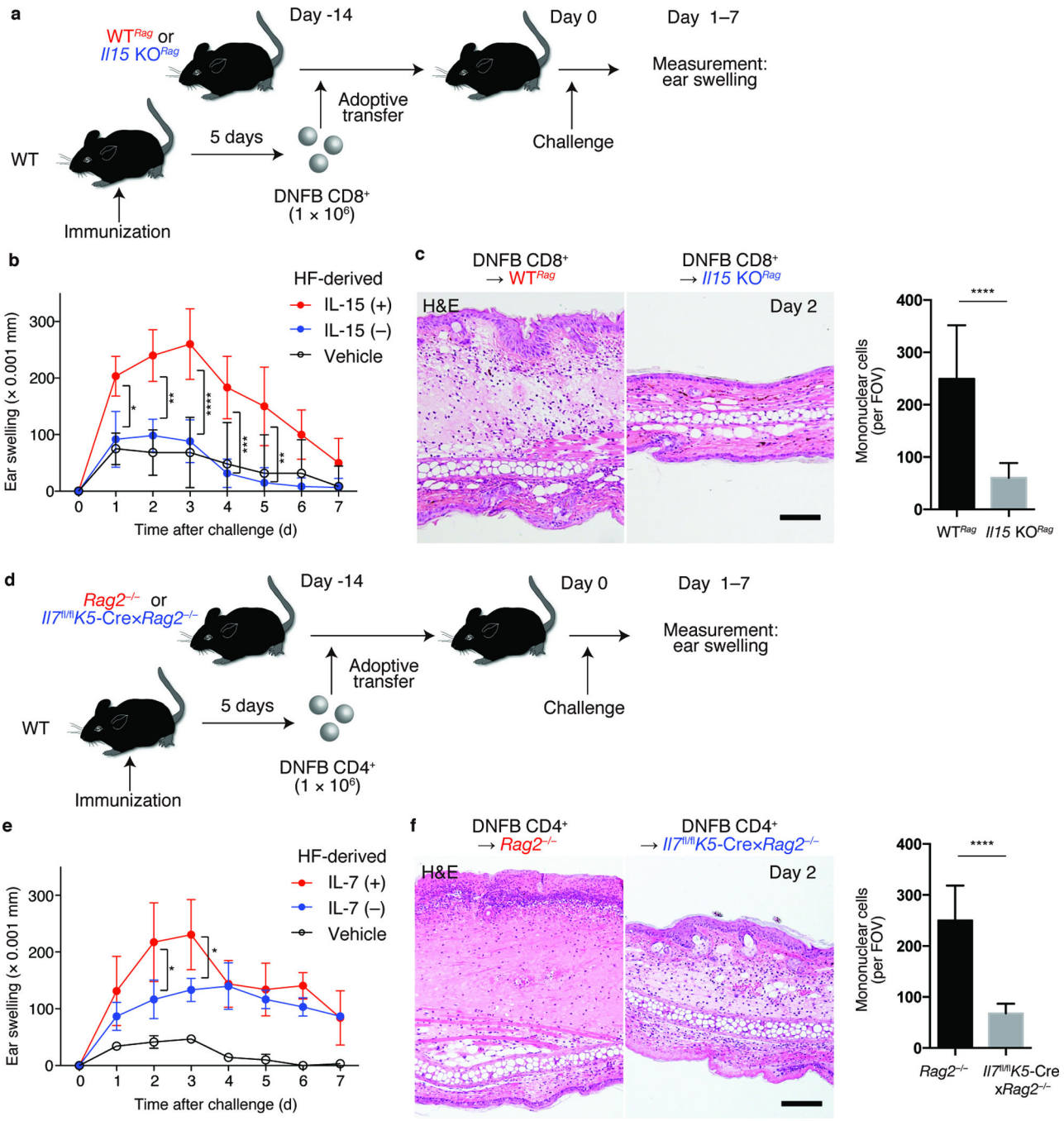

Figure 3. Impaired contact hypersensitivity responses in the absence of hair follicle-derived cytokines

(**a**) Experimental scheme for the analysis of $CD8^+$ T_{RM}-mediated CHS in the absence of peripheral tissue (hair follicle)-derived IL-15. $CD8^+$ T cells from DNFB (DNFB $CD8^+$) or vehicle-immunized (Vehicle $CD8^+$) WT mice were transferred into indicated lymphopenic mice. 14 days later, recipients were challenged with DNFB on their ears, and ear-swelling responses were measured. (**b**) Ear thickness (Δmm) of DNFB $CD8^+$-transferred WT^{Rag} (red), *Il15* KO^{Rag} (blue), and vehicle $CD8^+$-transferred WT^{Rag} (black) (n = 3). (**c**)

Hematoxylin and eosin staining of ear sections from indicated mice, day 2 after challenge and quantification of skin-infiltrating mononuclear cells. (**d**) Experimental scheme for analyzing $CD4^+$ T_{RM}-mediated CHS in the absence of hair follicle-derived IL-7. DNFB $CD4^+$ or vehicle $CD4^+$ were adoptively transferred into indicated lymphopenic mice. (**e**) Ear thickness (Δ mm) of DNFB $CD4^+$-transferred *Rag2*$^{-/-}$ (red), *Il7*$^{fl/fl}$*K5*-Cre×*Rag2*$^{-/-}$ (blue), or vehicle $CD4^+$-transferred *Rag2*$^{-/-}$ (black) (*n* = 3). (**f**) Hematoxylin and eosin staining of ear sections from indicated mice, day 2 after challenge, and quantification of skin-infiltrating mononuclear cells. Data are from one experiment, representative of two independent experiments with three mice per group in each (**b, c, e, f**). Cell counts represent pools of three fields of view per section (100×) from three mice per group (c, f). Scale bar, 100 μm (c, f). *P < 0.05, **P < 0.01, ***P < 0.001, ****P < 0.0001 (two way ANOVA).

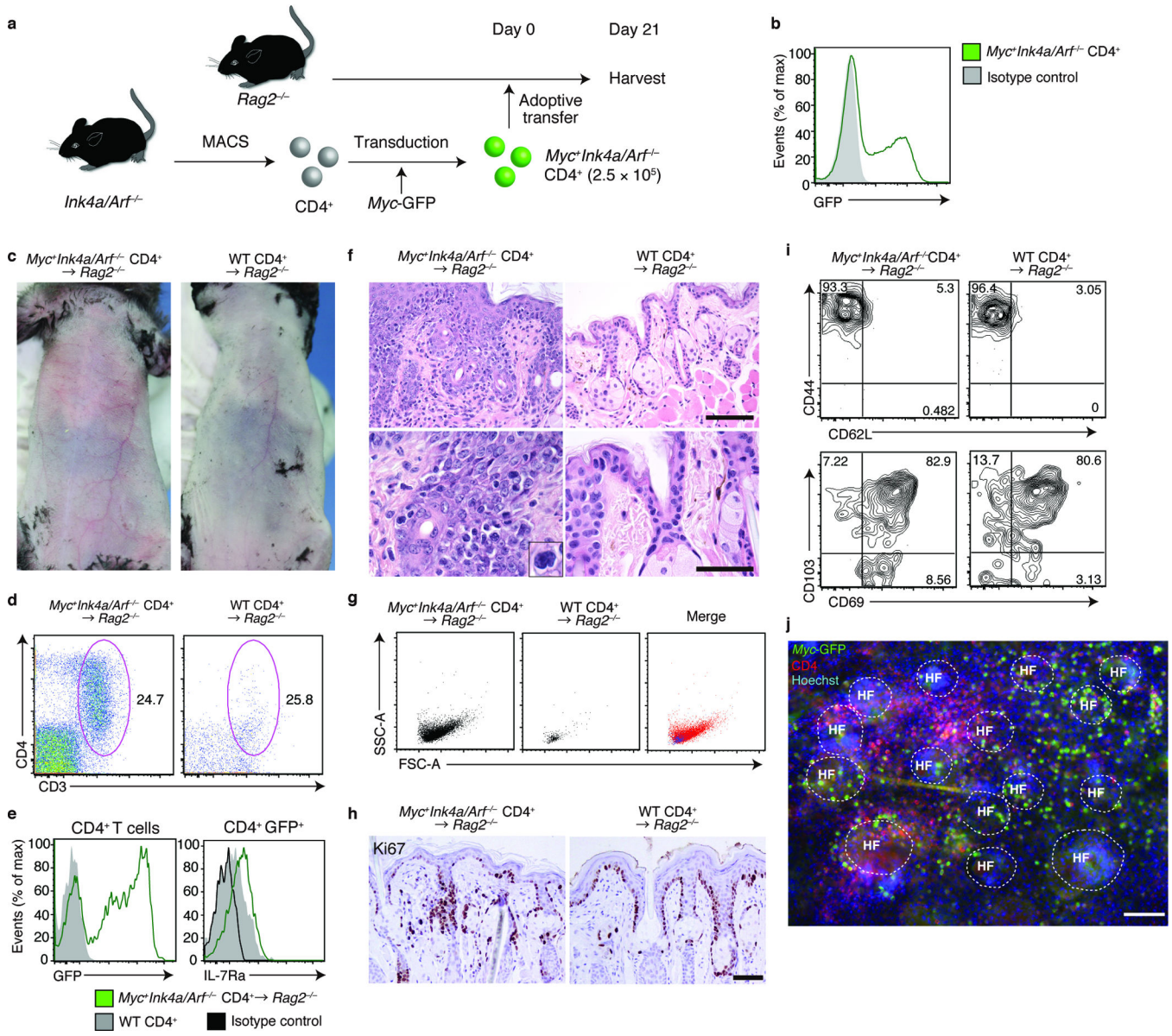

Figure 4. Generation of a model of T cell lymphoma with skin involvement

(**a**) Experimental scheme for a CD4$^+$ T cell lymphoma model with skin involvement. CD4$^+$ T cells isolated from *Ink4a/Arf*$^{-/-}$ mice were retrovirally transduced with *Myc*-GFP (*Myc*$^+$*Ink4a/Arf*$^{-/-}$ CD4$^+$) and were adoptively transferred into *Rag2*$^{-/-}$ mice. (**b**) Flow cytometry analysis of *Myc*-GFP expression on *Myc*$^+$*Ink4a/Arf*$^{-/-}$ CD4$^+$ T cells before transfer. (**c**) Skin phenotype of *Myc*$^+$*Ink4a/Arf*$^{-/-}$ CD4$^+$-transferred (left panel) or WT CD4$^+$-transferred *Rag2*$^{-/-}$ mice mice (right panel) (*n* = 3). (**d**) Flow cytometry analysis of CD3$^+$CD4$^+$ epidermotropic cells in indicated mice, for (**e**) expression of GFP and IL-7Rα, (**g**) forward and side scatter profiles, (**i**) CD44 versus CD62L and CD103 versus CD69 expression. Gated on CD45$^+$MHCII$^-$TCRγδ$^-$ (**d,g**), CD45$^+$MHCII$^-$TCRγδ$^-$ CD3$^+$CD4$^+$ (left panel in **e, i** and **j**) or CD45$^+$MHCII$^-$TCRγδ$^-$ CD3$^+$CD4$^+$GFP$^+$ populations (right panel in **e**) (*n* = 3). (**f**) Hematoxylin and eosin staining of lip sections from indicated mice and (h)

immunohistochemical staining for Ki-67 (n = 3). (**j**) Immunofluorescence microscopy of epidermal sheets, visualized for *Myc*-GFP, CD4 and Hoechst (n = 3). Scale bar, 100 μm. Data are from one experiment representative of three independent experiments with three mice per group in each.

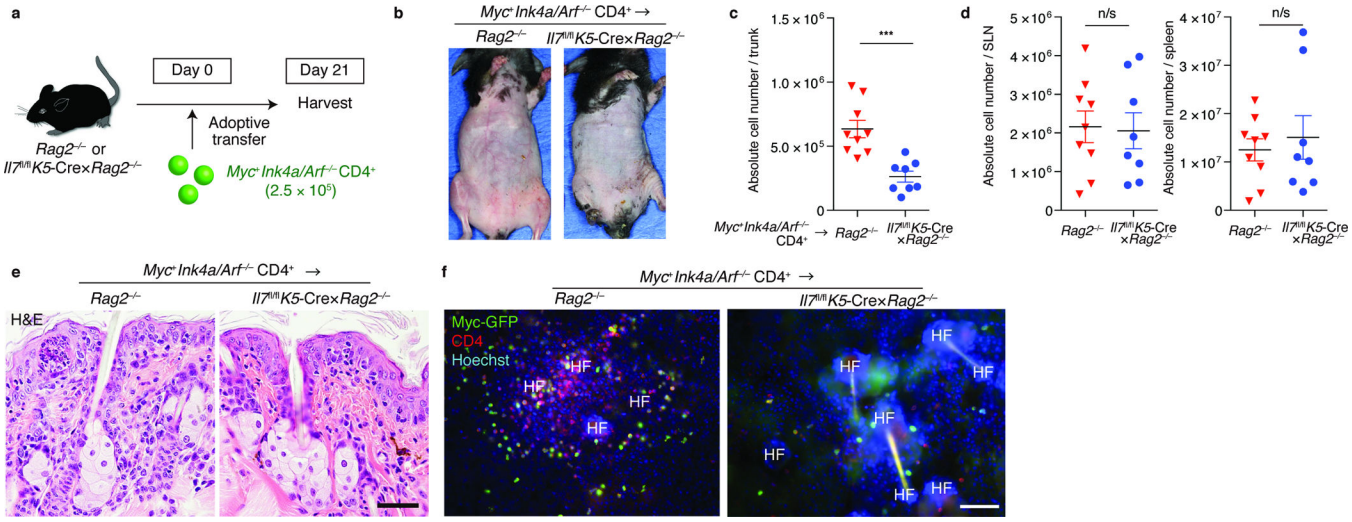

Figure 5. CD4$^+$ T$_{RM}$ lymphoma cells depend on hair follicle-derived IL-7 to exhibit epidermotropism

(**a**) Experimental scheme. *Myc*$^+$*Ink4a/Arf*$^{-/-}$ CD4$^+$ T cells were adoptively transferred into *Rag2*$^{-/-}$ or *Il7*$^{fl/fl}$*K5*-Cre×Rag2$^{-/-}$ mice. Recipient mice were harvested approximately three weeks after transfer. (**b**) Skin phenotype of recipient mice of indicated genotype (n = 3). Quantification of (**c**) epidermotropic T$_{RM}$ or (**d**) T cells in skin-draining LNs (SLN) and spleen, assessed at day 21 after adoptive transfer (n = 8–9). ***P < 0.001 (unpaired two-tailed Student's t-test). (**e**) Histology of skin sections from indicated mice, stained for hematoxylin and eosin, and (**f**) immunofluorescence microscopy of ear epidermal sheets of indicated mice, visualized for *Myc*-GFP, CD4 and Hoechst, assessed day 21 after adoptive transfer (n = 3). Scale bar, 100 μm. Data are from one experiment representative of three independent experiments with two to three mice per group in each (**b,e,f**) or an accumulation of three independent experiments (**c,d**).

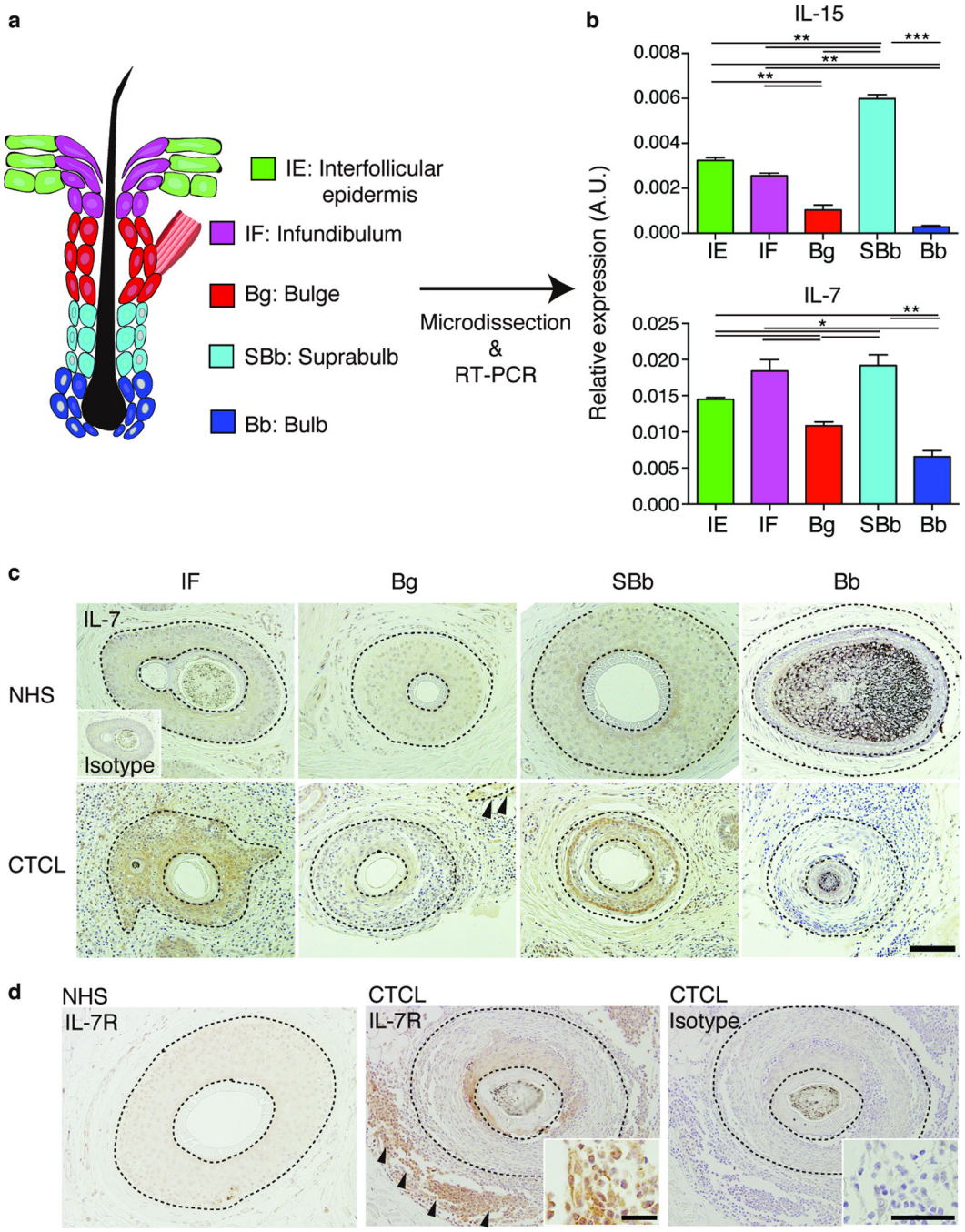

Figure 6. IL-7 and IL-15 expression in human hair follicles from normal scalp and cutaneous T cell lymphoma

(**a**) Schematic representation of human hair follicle keratinocytes. **(b)** Real-time PCR analysis for *IL15* and *IL7* expression at distinct sites in the hair follicle. *P < 0.05, **P < 0.01, ***P < 0.001 (unpaired two-tailed Student's *t*-test). (**c**) Immunohistochemistry of scalp sections from normal humans (NHS) (*n* = 3 samples from three subjects) and from subjects with CTCL (*n* = 6 samples from 3 subjects), stained with an anti-IL-7 antibody or with an isotype control. Scale bar, 100 μm. Arrowheads indicate arrector pili muscle (reflecting the

bulge region). (**d**) Immunohistochemistry of scalp sections from patients with CTCL, stained with an anti-IL-7R antibody or with an isotype control (n = 6 samples from three subjects). Scale bar, 100μm in low power field, 50 μm in high power field. Dashed lines delineate hair follicles. Arrowheads indicate IL-7R-positive lymphoma cells. Data are from one experiment representative of three (**b,c**) or two (**d**) independent experiments.